



## Article

# Synchronization of Monostatic Radar Using a Time-Delayed Chaos-Based FM Waveform

Mariam H. Abd <sup>1</sup>, Ghaida A. Al-Suhail <sup>2</sup> , Fadhil R. Tahir <sup>3</sup>, Ahmed M. Ali Ali <sup>4</sup> , Hamza A. Abbood <sup>5</sup>,  
Kia Dashtipour <sup>6</sup> , Sajjad Shaukat Jamal <sup>7</sup> and Jawad Ahmad <sup>6,\*</sup>

<sup>1</sup> Department of Engineering Works, Infrastructure Directorate, Al Nasiriya 64001, Iraq; mariam876am@gmail.com

<sup>2</sup> Department of Computer Engineering, College of Engineering, University of Basrah, Basrah 61001, Iraq; ghaida\_alsuhail@yahoo.com

<sup>3</sup> Department of Electrical Engineering, College of Engineering, University of Basrah, Basrah 61001, Iraq; fadhilahma@hotmail.com

<sup>4</sup> Department of Electronics Techniques, Babylon Technical Institute, Al-Furat Al-Awsat Technical University, Babylon 51001, Iraq; ahmed.ali@atu.edu.iq

<sup>5</sup> Production Department, Petro China International Iraq, FZE Iraq Branch, Maysan 62008, Iraq; hamza.abd.k@gmail.com

<sup>6</sup> School of Computing, Edinburgh Napier University, Edinburgh EH10 5DT, UK; k.dashtipour@napier.ac.uk

<sup>7</sup> Department of Mathematics, College of Science, King Khalid University, Abha 61413, Saudi Arabia; shussain@kku.edu.sa

\* Correspondence: j.ahmad@napier.ac.uk

**Abstract:** There is no doubt that chaotic systems are still attractive issues in various radar applications and communication systems. In this paper, we present a new 0.3 GHz mono-static microwave chaotic radar. It includes a chaotic system based on a time-delay to generate and process frequency modulated (FM) waveforms. Such a radar is designed to extract high-resolution information from the targets. To generate a continuous FM signal, the chaotic signal is first modulated using the voltage control oscillator (VCO). Next, the correct value for the loop gain (G) is carefully set when utilizing the Phase-Locked Loop (PLL) at the receiver, so that the instantaneous frequency that reflects a chaotic state variable can be reliably recovered. In this system, the PLL synchronization and radar correlation are enough to recover the echo signal and detect the target. The finding indicates that the system can be implemented with no need to use the complete self-synchronization or complex projective synchronization schemes as compared to the existing chaotic radar systems. The simulation results show that the short-time cross-correlation of the transmitted and reconstructed waveforms is good and satisfactory to detect the target under various signal-to-noise ratio (SNR) levels and with less complexity in the design.

**Keywords:** synchronization; chaotic time-delay; Phase-Locked Loop (PLL); mono-static radar; Chaotic FM Radar



**Citation:** Abd, M.H.; Al-Suhail, G.A.; Tahir, F.R.; Ali Ali, A.M.; Abbood, H.A.; Dashtipour, K.; Jamal, S.S.; Ahmad, J. Synchronization of Monostatic Radar Using a Time-Delayed Chaos-Based FM Waveform. *Remote Sens.* **2022**, *14*, 1984. <https://doi.org/10.3390/rs14091984>

Academic Editors: Dmitry Garmatyuk and Chandra Sekhar Pappu

Received: 24 February 2022

Accepted: 15 April 2022

Published: 20 April 2022

**Publisher's Note:** MDPI stays neutral with regard to jurisdictional claims in published maps and institutional affiliations.



**Copyright:** © 2022 by the authors. Licensee MDPI, Basel, Switzerland. This article is an open access article distributed under the terms and conditions of the Creative Commons Attribution (CC BY) license (<https://creativecommons.org/licenses/by/4.0/>).

## 1. Introduction

After decades of research, the chaotic signal is experiencing rapid development in many fields, such as engineering and science. In a variety of applications, chaotic signals have been observed, including mechanics, electronics, chemistry, and acoustics. Since it owns many of the features that distinguish it, such as the chaotic signal random-in-time involvement with no periodicity, but rather the signal energy is distributed across all ranges of frequency and a chaotic signal can be generated from simple chaotic deterministic systems, the noise-like and complex behavior of a chaotic signal could have advantages in various fields of practical applications, such as being used in radar systems [1–3]. This feature of the chaotic signal makes the radar signal simple to implement, less sensitive to jamming or interference, and easy to process.

Typically, chaotic signal (CS) is characterized as a deterministic broadband signal, has a structure, and the maximum Lyapunov exponent is greater than zero; meanwhile the noise is expressed as a random and non-deterministic signal [3]. As CS has distinct characteristics of unsystematic phase variation and broadband of power spectrum, so chaos radars can easily offer the key characteristics:

- Chaotic signal using simple and inexpensive deterministic systems.
- CS has featureless low-probability of intercept/low probability of detection (LPI/LPD) characteristics, and therefore it is hidden or invisible signal.
- CS is inherently anti-jamming signal and interference resistant.
- CS is spectrally very efficient and can share spectral bands without any mutual interference. Then chaotic radar may utilize coherent signal processing schemes either by matched filter or correlation in order to reduce the noise in the echo signal and detect the target successfully.

In general, in radar systems, there are a number of transmitter/receiver (antenna) nodes that are designed to make the system operate either as monostatic, bistatic, or multistatic radar. Each radar system depends on the type of waveform, whether continuous or non-continuous (i.e., pulse wave) [2]. The radar is called monostatic radar if the transmitter and receiver are placed in the same place; otherwise, the radar is a bistatic or multistatic type if both transmitter and receiver(s) are separately located over a distance [4]. Figure 1 depicts the three types of radar systems.

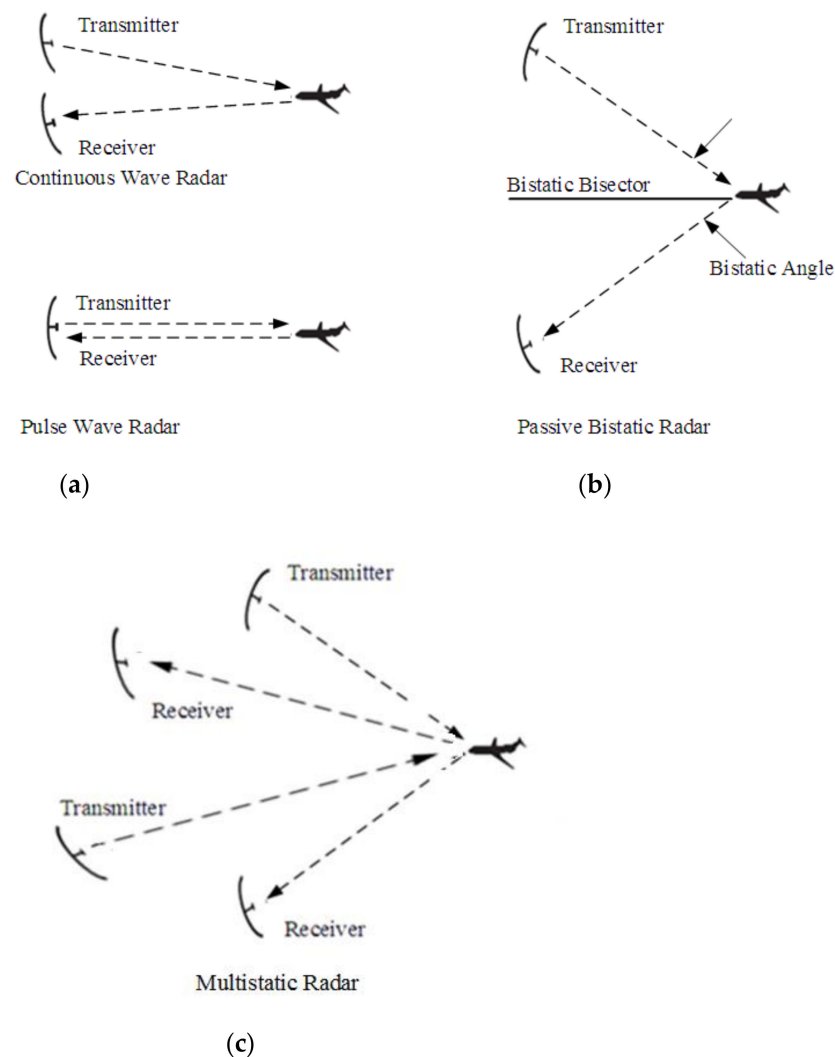


**Figure 1.** A type of radar systems (a) Monostatic (b) Bistatic and (c) Multistatic radars.

However, the major drawback in these passive bistatic radars mainly suffers from the lack of control on the transmitting waveform. Meanwhile, the conventional monostatic defense radars have a shortage in detecting low radar cross-section (L-RCS) targets. Figure 2 illustrates the fundamental operation of mono-static radar systems. In fact, the RCS metric is the crucial measure that defines the reflectivity of the target measure; thus, a larger RCS means easier target detection because the RCS of any target depends on the radar's transmitted frequency. Thus, the long-wave radars (below HF) have more precision, with large RCS compared to HF, VHF, and UHF radars. More details are presented in [2,5,6]. However, most conventional radars are basically designed to operate on the microwave frequency band between 300 MHz (1 m) and 300 GHz (1 mm). On the other hand, several chaos radar systems have been designed and implemented for various secure communications [7–10]; they may employ coherent signal processing schemes either by matched filter or correlation to reduce the noise and eventually obtain the highest improvement in Signal-to-Noise Ratio (SNR) [7,11]. Another issue in chaotic based radar systems (CBRS) is choosing the type of chaos synchronization between the transmitter and the receiver nodes. Conversely, traditional synchronization schemes such as Phase-Locked Loop (PLL) can be used in chaotic radars [4]. In fact, there are many studies on complete synchronization and feedback control [7,8] in a radar system, but the limitation is raised due to its sensitivity to noise, and any tiny amounts of additive noise to the (echo) signal can degrade the synchronization quality, and the chaotic signals may not be synchronized [11].

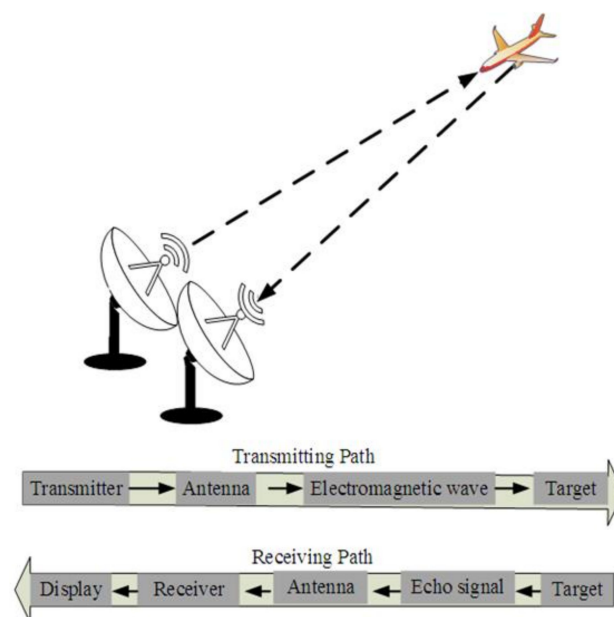


**Figure 2.** A general principle of the simple monostatic continuous radar system.

Moreover, some CBRS systems have been widely studied, either with no modulation, such as pulse compression, or within a variety of modulation methods, such as continuous AM/FM/PM modulation where many CBRSs are utilized in microwave and UWB and laser applications [4,12,13]. One example was devoted to a microwave chaos signal practically generated through the Colpitts oscillator and directly transmitted through a wide-band antenna without modulation [7,8]. In this paper, therefore, the key issue is how to design a robust chaotic radar system that can provide a complete- or quasi-synchronization in order to successfully recover the echo signal and then detect the target. To achieve this goal, we present a new robust indirect mono-static FM-based chaos radar using a time-delayed chaotic system under various levels of noise over the wireless channel. The design is simple and it does not need to use the complete self-synchronization or any complex projective synchronization schemes.

The following is a breakdown of the paper's structure: Section 2 introduces an overview of the frequency band design of radar systems and stealth counters. Section 3 explains the chaos radar challenges and the main contribution in this study. Section 4 addresses some related works on chaotic radars. The dynamical analysis of the mathematical model of the first-order time-delay chaotic system, as well as its dynamical properties such as the phase portrait chaotic attractor, equilibrium points, Nyquist plot, and bifurcation diagram, are presented in Section 5. Section 6 describes the chaotic signal based on FM modulation and how to modulate the chaotic signal with the voltage control oscillator (VCO) to generate continuous FM signals and then recover the reference signal with the PLL. Section 7 explains the comparative performance with the existing chaotic radars. Finally, Section 8 summarizes the conclusions and perspectives of this paper.

## 2. Radar Systems and Stealth Counter: Overview

Obviously, the design of radar systems mainly depends on the desired band and the purpose of applications in civil or military communications. The usual microwave radars are often used from 2 GHz up to 40 GHz, and among these are Ultra-Wide Band (UWB) radars. Meanwhile, the low-frequency radars frequently use lower bands less than 1 GHz, such as L-band (1–2 GHz), UHF, VHF, and HF bands. Other types are called LiDAR (Light Detection and Ranging) or Laser Radars. These radars use visible, ultraviolet, or near-infrared radiation to detect targets. Ultrasound and sonar systems, on the other hand, use acoustics (audio and speech) waveforms. Specifically, the relatively large antennas often use frequencies within a bandwidth of 270 MHz (as VHF (30–300) MHz) or 700 MHz (as UHF (300 MHz–1 GHz)) to achieve narrow beams that may experience interference as they propagate through the ionosphere.

Small antennas, on the contrary, may be employed with weather radars in the S (2–4) GHz, C (4–8) GHz, X (8–12) GHz,  $K_u$  (12–18) GHz, and K (18–27) GHz bands to produce narrow beams and good range resolution. Skywave and Ground wave radars are the two forms of Over-the-Horizon (OTH) radars, respectively. Ground-wave radars can identify targets at very long range, often between (100 and 1000) km. They also operate at low frequencies (below 3 MHz), and therefore they suffer from diffraction due to the surface of the earth. Longwave bands in HF band (3–30) MHz employ Skywave (shortwave), where the short wave depends on the ionosphere [2,4–9,14].

On the other hand, the stealth counter has become an important topic in recent years to minimize the effectiveness of Radar Cross-Section (RCS) measures, and this requirement remains an open challenge in radar system design. Stealth is used to prevent detection systems under work by utilizing the electromagnetic spectrum, such as making the RCS small or through changing the shape of the aircraft, by using Radar Absorbing Material (RAM), or by utilizing the plasma which attenuates the radar energy. However, at high radar frequency, the attenuation effect of the plasma becomes greatest, while at VLFs it may be reflected by the plasma. Blessedly, most radar systems that aircraft are required to defend against operate in the X and  $K_u$  frequency bands. However, the design aim of the Low Observable (L.O.) or stealthy aircraft in the X and  $K_u$  bands is to reduce radar emission energy. At lower frequency bands, the RCS of L.O. aircraft must be increased, and the RAM use for the target is not so efficient in these bands. Therefore, this results in a serious interest in working on anti-stealth capabilities in radar systems [5,6].

Notably, during the Kosovo war in 1999, for example, the old VHF (also known as low frequency) radar was utilized to shoot down an F-117 Nighthawk by Serb forces [8,9]. Since 2013, several new radars for military and secure communications have been developed, including multitoned harmonic non-linear radar, US Navy Re-Locatable Over-the-Horizon Radar (ROTH), and OTH radar. Regardless of the target's altitude, they can identify stealthy and small targets at very long ranges. Although such radars have disadvantages, such as massive antennas, immobility, and a large quantity of clutter, they are nonetheless highly effective against stealth ships and stealth aircraft when deployed on the ground [9,10,14].

Additionally, the radar systems have also been linked with modern infrared for search and tracking (IRST) systems to provide anti-stealth capabilities in secure communications and the military. The IRST system actively scans the airspace for heat signatures, transmitting its IR emission, and passively detects and tracks the target based on IR emission, allowing the crew to attack without warning the target (i.e., first look then shoot). The IRST21 sensor in the F-14D Tomcat and the IRST in the super Hornet are two examples of current systems that are now in low production and could be operational by 2018, as shown in Figure 3 [6,15].

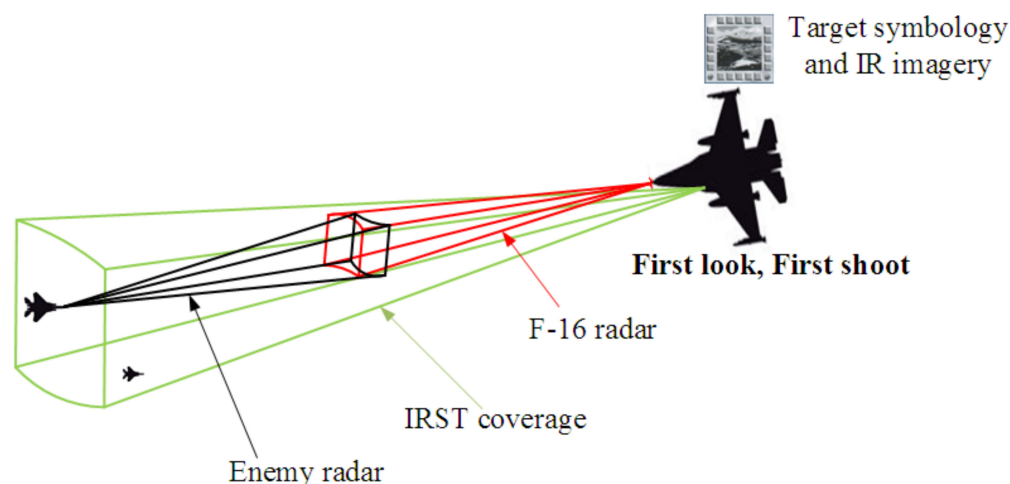


**Figure 3.** An example of a modern stealth Radar and IRST.

### 3. Chaos Radar Challenges

There are some challenges and problems facing the chaos radar systems that can be summarized as follows:

1. The key challenge is to build an easy, low cost, and more secure chaotic radar system, but this may result a complex behavior. The challenge for chaotic waveforms is whether these properties are adequate to provide unique and operant radar implementations.
2. The parameters mismatch in chaotic systems is still unavoidable in real situations of chaos synchronization. If the drive-response systems are not identical and there is a parameters mismatch, the synchronization error does not definitely converge to zero or it may lead to small fluctuations about zero; this is called quasi-synchronization or asymptotic synchronization [16]. Otherwise, loss of synchronization may occur in case of large parameters mismatch. Therefore, to design accurate synchronization with reasonable precision between the transmitter and the receiver, it is necessary to consider the role of parameters mismatch in the synchronization process.
3. Moreover, the relationship between chaos synchronization in time-delayed feedback systems and parameters mismatch is also another quite complex issue.

To the best of our knowledge, some studies [17,18] are only concerned with the coupled systems without time delay in the presence of parameters mismatch. Other significant reports have also been devoted on the adaptive-observer synchronization schemes to solve this problem using different time-delay chaotic systems [2–19]. Among these, Liu et al. [16], He et al. [19] and Huang et al. [20] have discussed some approaches on synchronization of two coupled delayed systems with parameters mismatch under particular certain coupling strength for the delayed Lur'e systems.

Upon these challenges, one of the solutions for the synchronization in the CBSR system is the Voltage-Control-Oscillator (VCO), which can be used for FM modulation in radar applications and by converting the frequencies of a base-band chaotic source system to microwave frequencies. The output frequencies are linearly changed with applied

input to VCO and the constant amplitude of the output microwave-signal. The frequency modulation method (FM) describes many characteristics such as the low eventuality of interception or detection in a radar system, the lower effect of jamming or noise, and less interjecting with other channels [4,10]. The authors focused on microwave chaos signal practically created by the Colpitts oscillator and directly sent through a wide-band antenna without modulation, since direct (i.e., without modulation) chaotic radar remains a major system in the research field [3,7].

Referring to the essential design criteria for a chaotic radar system, the main contributions in this study are summarized as follows:

- A new 0.3 GHz mono-static microwave chaotic radar is proposed based on a time-delay to generate and process frequency modulated (FM) waveforms. Tuning the right value for the loop gain ( $G$ ) is carefully set in the Phase-Locked Loop (PLL) in order to reflect more reliable signal recovery.
- The finding indicates that such a radar system can be implemented with no need to complete self-synchronization or complex projective synchronization.
- Obtained results reveal the robustness of chaotic monostatic radar under various noise levels in terms of short-time cross-correlation of the transmitted and reconstructed waveforms.
- The proposed indirect mon-static chaotic radar system is considered as a state-of-the-art in a secure communication application.

#### 4. Related Work

Synchronization of chaotic systems is an interesting scheme and is studied in many research engineering applications. The first savant studied the synchronization between two identical systems without the same initial condition by Pecora and Carroll (PC) in 1990 [21]. Several control methods have been devoted to the chaotic signal in order to make the synchronization between two systems (master–slave), such as Ott et al. who, in 1990, first presented the scheme of chaos control [22], sliding mode control method [23], adaptive control method [24], impulsive control method [25], back-stepping design method [26], sampled-data feedback method [27], and other methods for control on synchronization of the chaotic signal [28]. This method and other methods have been proposed to make different chaotic systems stabilized around the unstable orbit. One example is finite-/fixed-time synchronization of memristor chaotic systems (MCSs), which are addressed via the sliding-mode control method in image encryption applications [29].

On the other hand, Chandra et al., in [4], introduced chaos-based frequency modulated (CBFM) waveforms for joint monostatic and bi-static radar-communication systems, and the wideband radar imaging uses short-duration pulses created by chaotic oscillators, with the information contained in the pulses using chaos shift keying (CSK). The information is decoded at the communication receiver, and the transmitted waveform is reconstructed at the bistatic radar receiver, using a self-synchronization technique for chaotic systems, and it is shown that the CBFM waveforms closely track the theoretical Bit-Error Rate (BER) associated with bipolar phase-shift keying using a nonlinear detection approach (BPSK). At the bistatic radar receiver; the same nonlinear detection approach is used to optimize target detection. In both the monostatic and bistatic examples, the ambiguity function resembles a thumbtack ambiguity function with a pseudo-random side lobe distribution. In addition, Al-Suhail et al. [2] proposed a direct monostatic radar model using a chaotic time-delayed system in the presence of self-synchronization to recover the echo signal for long-wave anti-stealth applications. To overcome the problems encountered in VLF chaos radar design, such as parameters mismatch of chaotic system in chaos synchronization, in this paper, we developed the FM-based chaotic radar system (0.3 GHz). The Phase-Locked Loop (PLL) is used in place of Pecora and Carroll (PC) or an adaptive-observer scheme in order to achieve chaos synchronization and then recover the original signal correctly. The master chaotic signal (source) is transmitted via the VCO to convert the baseband signal to a microwave signal; after that, it is transmitted through a wireless channel with echo delay

and under various values of noise levels. Then, the received echo signal is demodulated by the analog Phase-Locked Loop (PLL) to recover the reference signal, and the correlation is used to measure the performance of the proposed mono-static radar system.

### 5. Design of Time-Delay Chaotic Systems

In this study, chaotic behavior in a dynamical system with a single state variable and a minimum number of elements is addressed in detail using a simple time-delay chaotic system in Lur'e form. The Lur'e system consists of three elements, namely time-delay, an integrator, and non-linearity, respectively, as shown in Figure 4. The time-delay affects the dynamic of the systems, such as single state time-delay, which makes the system infinite-dimensional, the integrator officiates the system dynamics of a single state, and the non-linearity is a necessary part and is wanted as a major, so chaos is a distinguishing characteristic of nonlinear systems [30,31]. Consequently, the dimensionless equation of the Lur'e system can be expressed as follows

$$\dot{x}(t) = k[-ax(t) - bF(x_\tau)] \tag{1}$$

where  $x(t) \in \mathbb{R}$  is the state variable,  $x_\tau = x(t - \tau)$ ,  $F(\cdot) : \mathbb{R} \rightarrow \mathbb{R}$  is a non-linear function,  $\tau \in \mathbb{R}^+$  is the time-delay,  $k$  is the scaling factor, and  $a$  and  $b$  are system parameters. The non-linearity is multiplied by the gain  $b$ , whilst the pole of the Miller integrator is  $ka$ . The Lur'e form in system (1) consists of two parts: the linear part given by  $L(s) = \frac{ke^{-s\tau}}{s + ka}$  and the feedback nonlinear part given by  $\mathcal{N} = bh(x)$  [30,32].

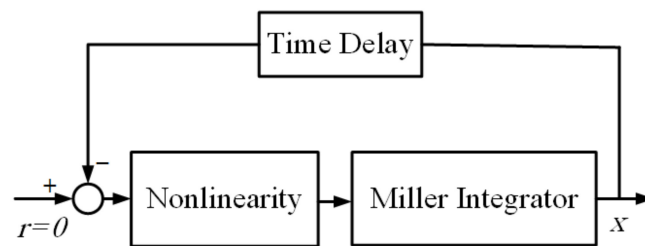


Figure 4. The Lur'e system's structure.

To observe the chaos from a Lur'e system, three conditions must be satisfied: (a) the existence of a stable predicted limit cycle (PLC) and a separate unstable equilibrium point, (b) the interaction between the stable predicted limit cycle and the unstable equilibrium points, and, finally, (c) the linear part of the Lur'e system must be filtering. In our system, it is always satisfied, since  $L(s) = \frac{ke^{-s\tau}}{s + ka}$ .

Due to the piecewise linear nonlinearity under consideration, the condition of the PLC is investigated. The harmonic balance approach [32] can be used to determine the existence of stable PLC. A limit cycle (LC) solution of type  $Y_0(t) = A\sin(\omega t)$  exists if the amplitude  $A$  of  $Y_0$  satisfies the following equation:

$$1 + L(j\omega)N(A) = 0 \tag{2}$$

where  $N$  is the static describing the function of nonlinearity  $\mathcal{N}$ . The intersection points between the curve  $L(j\omega)$  and the curve  $-1/N(A)$  in the complex plane can be used to determine the solution to the system (2). Each intersection represents LC at a specific frequency and amplitude. The LC is considered unstable if the intersection points along the curve  $-1/N(A)$  are encircled by the curve  $L(j\omega)$ . Otherwise, the LC is stable.

The existence of unstable equilibrium points that are separate from the PLC is required by the second condition. With a double scroll, the chaotic attractor can be generated from the system (1), and the PWL function is defined by

$$F(x_\tau) = x_\tau - \text{sgn}[x_\tau] \tag{3}$$

Hence, a sawtooth wave can be seen in the PWL function in the system (3). Now, using systems (1) and (3), the following equation can be used to locate equilibrium points:

$$k[-ax(t) - bF(x_\tau)] = 0 \tag{4}$$

As shown in Figure 5, the three equilibrium points  $\pm x_i^e$  ( $i = 0, 1$ ) are located at the intersection of  $F(x_\tau)$  and  $x$ .

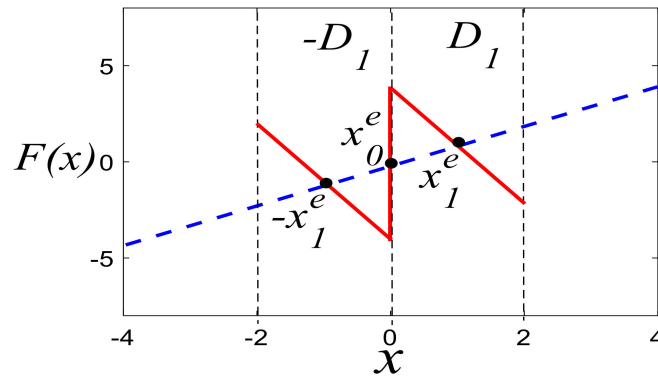


Figure 5.  $F(x_\tau)$  and its characteristic regions of chaotic 2–scroll attractor.

Only the situation  $x \geq 0$  needs to be considered because of the symmetry of the function  $F(x_\tau)$ . Obviously, based on the linear regions of the characteristic equation, the system (1) with (3) can be classified into many linear regions  $\pm D_i (i = 1)$ .

From the symmetry of the function  $F(x)$ , one only needs to consider the case  $x \geq 0$ . Obviously, the system (1) with (3) can be classified into several linear regions ( $\pm D_i (i = 1)$ ) based on the linear regions of the characteristic equation.

Figure 6 depicts the bifurcation diagram of this system with respect to  $\tau$ . The equilibrium points (zeroes of PWL functions defined by Equation (3)) are stable for  $\tau < 0.45$  ms, and the trajectory of the system (1) converges with it, with no PLC occurring in this case. When the time delay ( $\tau$ ) is increased until it reaches  $\tau \geq 0.45$  ms, chaos occurs, because the LC is expected and begins to interact with unstable equilibrium points [30]. Notably, this time-delayed system was successfully implemented using OrCAD PSpice Designer and illustrated for different multi-scrolls by Fadhil et.al. in [30].

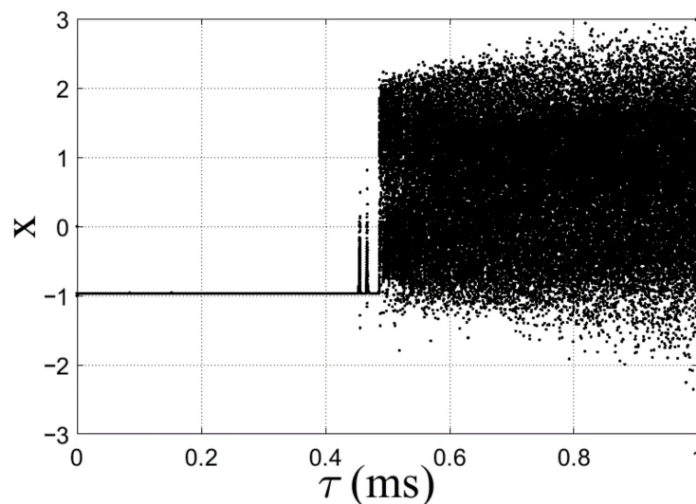


Figure 6. The bifurcation diagram of the system (1) with nonlinearity (3) as a function of time delay  $\tau$  for system parameters  $a = 1$ ,  $b = 2.6$ , and  $k = 1800$ .



Through the graphical solution (2), the dynamic of the system is represented in terms of the conditions for the existence of chaos for  $\tau = 0.6$  ms,  $a = 1$ , and  $k = 1500$ , and the Nyquist plot of  $L(j\omega)$  intersects the curve  $-1/N(A)$ , as shown in Figure 7. It leads to a stable PLC and the system behaves chaotically. Except for the equilibrium points, any number in the basin of attraction can be used as the initial condition for the system (1). The parameter values of the system (1) can be selected as  $a = 1$ ,  $b = 3$ , has a chaotic attractor with PWL nonlinearity (3), and  $x(0) = 0.5$  and  $\tau = 0.6$  ms, as shown in Figure 8. In fact, the phase trajectory over time is clearly shown in this figure, where a chaotic signal can introduce various attractors once the time delay is changed [33]. Similarly, in [34], Li et al. showed that a chaotic oscillator utilizing a flux-controlled memristor can also produce various signals with increasing amplitude and frequency for the broad requirements in engineering applications.

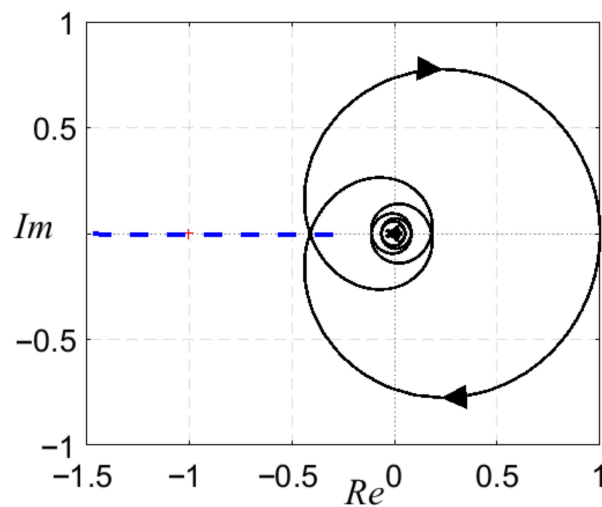


Figure 7. A graph of the equation’s solution (2). The dashed line is the function  $-1/N(A)$ , whereas the continuous curve is a Nyquist plot of  $L(j\omega)$  with  $\tau = 0.6$  ms.

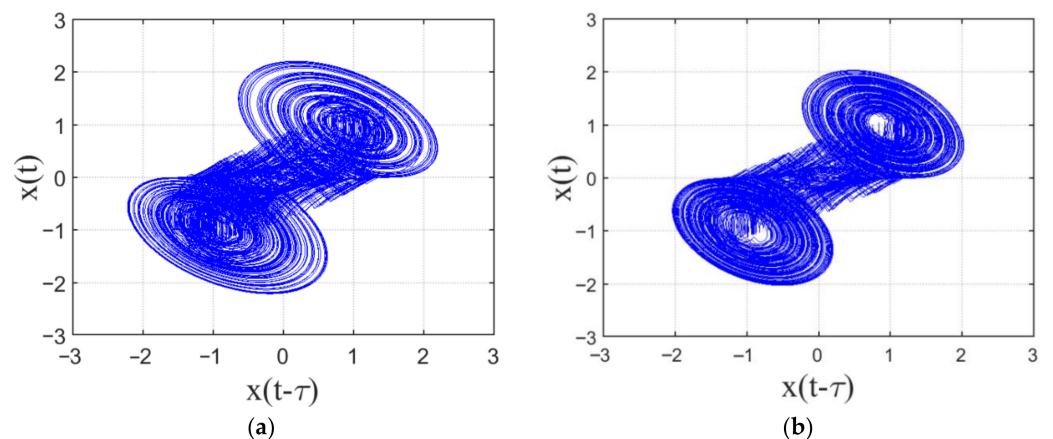
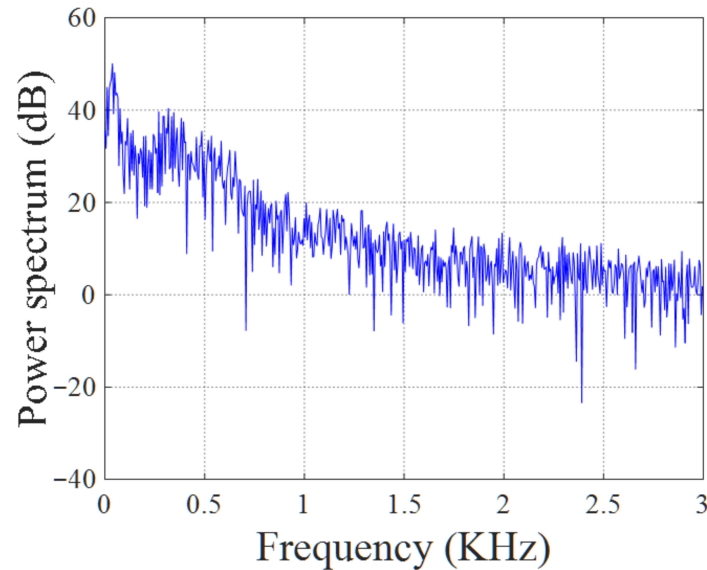


Figure 8. Chaotic attractors for  $x(0) = 0.5$ ,  $\tau = 0.6$  ms,  $a = 1$ ,  $b = 3$ , and  $k = 1500$ . (a) Time delay  $\tau = 0.6$  ms, (b) time delay  $\tau = 0.5$  ms.

Accordingly, system (1) with the selected parameter values  $a = 1$ ,  $b = 2$ , and  $k = 1800$ , and  $x(0) = -1$  can also produce the delay-dependent chaotic attractor with double scrolls at the time delay  $\tau^* \geq 0.45$  ms. It means that  $\tau$  has a significant effect once this delay has been increased, leading to different delay-dependent double-scroll attractors. Hence, the more complex chaotic behavior of  $\tau \geq 0.6$  ms indicates the more complex attractors generated with different amplitude and frequency in order to meet more secure communication, especially in chaotic radar applications [33].

Note that the output signal obtained from the dynamical Lur'e system in Figure 4 is characteristic of the broad band chaotic spectrum. The Fast Fourier Transformer (FFT) is applied on the chaotic signal. Then, the power spectrum of the output signal  $x(t)$  can be obtained, as shown in the Figure 9, for the time delay  $\tau = 0.6$  ms and sampling frequency  $f_s = 4$  MHz. This base band spectrum deploys below the frequency range of 3 kHz. Thus, the chaotic signal is classified with a Very-Low Frequency (VLF) chaotic band, and such a feature allows direct long-wave chaotic radar system to be built for anti-stealth applications [2].



**Figure 9.** The power spectrum frequency of the output signal from Lur'e system with time delay  $\tau = 0.6$  ms and sampling frequency  $f_s = 4$  MHz.

## 6. Chaotic Signal-Based on FM Modulation

After we generated the chaotic attractor from the time-delay chaotic system in Section 5, we could use it in the FM modulation. Thus Figures 10 and 11 show the chaotic signal's modulation and demodulation structures, respectively. The voltage control oscillator (VCO) is used to modulate the chaotic signal and generate continuous FM signals. The low-pass filter (LPF) receives the output signal from the time-delay chaos source block (the master signal  $x(t)$ ) and assuming the cutoff frequency of LPF ( $f_{cut} = 1$  MHz), first-order, and with the Butterworth method). Then, the limited chaotic master signal ( $x_m(t)$ ) is regarded as an input signal to the VCO during the modulation process. Then, the output signal from the VCO becomes a transmitted signal ( $S_t(t)$ ) through wireless channel [4,35].

$$S_t(t) = A \cos[2\pi f_c t + 2\pi K_{vco} \int_0^t x_m(t) dt] \quad (5)$$

where the carrier frequency is  $f_c$  and the sensitivity of the VCO in Hz/V is  $K_{vco}$ , and

$$K_{vco} = \frac{f_{max} - f_{min}}{v_{max} - v_{min}} = \frac{BW}{v_{max} - v_{min}} \quad (6)$$

where  $f_{min}$  and  $f_{max}$  are the minimum and maximum frequency, while  $v_{min}$  and  $v_{max}$  denote the minimum and maximum voltages of  $x_m(t)$ , respectively. The difference between maximum and minimum frequencies has represented the bandwidth ( $BW = f_{max} - f_{min}$ ) of the modulated signal and the instantaneous frequency deviation described in the term  $K_{vco} x_m(t)$ . The nonlinear frequency relation is between the input of the master signal to VCO and the transmitted signal ( $S_t(t)$ ), as noted in Equation (5). The received signal  $\hat{S}_t(t)$  is demodulated by the analog Phase-Locked Loop (PLL), as shown in Figure 11.

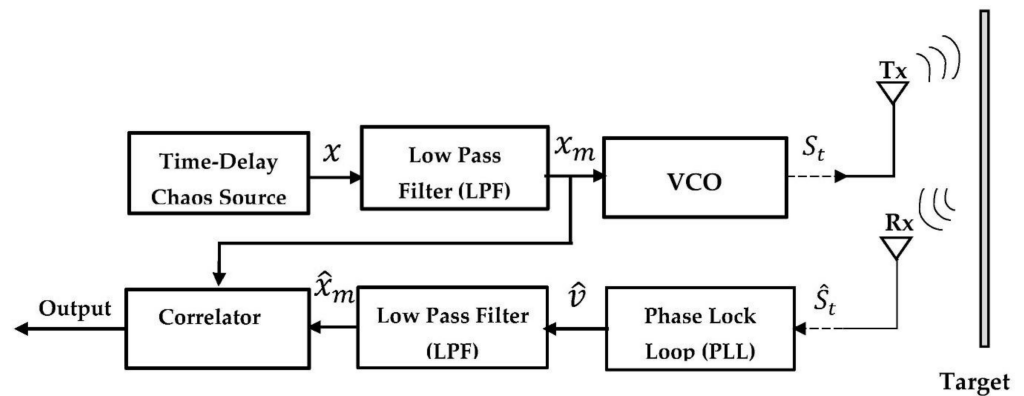


Figure 10. The block diagram of a Time-delayed Chaotic-FM Radar System.

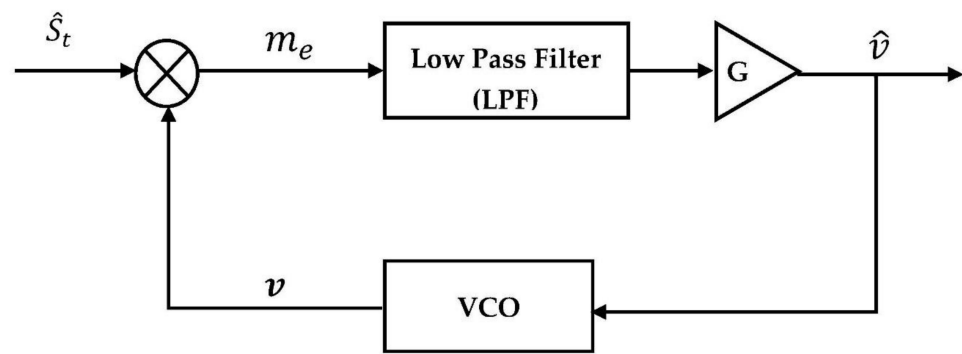


Figure 11. The structure of signal demodulation using PLL.

As shown in Figure 11, a PLL consists of three components: a VCO, a low pass filter (LPF), and a mixer. Here, the LPF is built with  $f_{cut} = 150$  MHz, first order, Butterworth method. The phase detector (PD) acts as a mixer to compare the phase of the received signal  $\hat{S}_t(t)$  with the phase of the VCO. The output signal of PD represents the error voltage  $m_e(t)$ , which is filtered by the loop LPF. However, this signal is amplified by the loop gain  $G$  and is assumed to produce  $\hat{v}(t)$  that later feeds the VCO. Subsequently, the output signal from the VCO ( $v(t)$ ) is multiplied by the received signal  $\hat{S}_t(t)$  to obtain  $m_e(t)$ . Then, the output of the VCO is described as [4,35,36]:

$$v(t) = V_r \sin(\theta_v) \tag{7}$$

where,

$$\theta_v = 2\pi f_c t + 2\pi K_{vco} \int_0^t \hat{v}(t) dt \tag{8}$$

$$m_e = \hat{S}_t * v(t) \tag{9}$$

and the voltage amplitude of the VCO output signal is  $V_r$ . Then, the output of the LPF can be described by

$$\hat{v}(t) = \frac{1}{2} \sin(\theta_t - \theta_v) \tag{10}$$

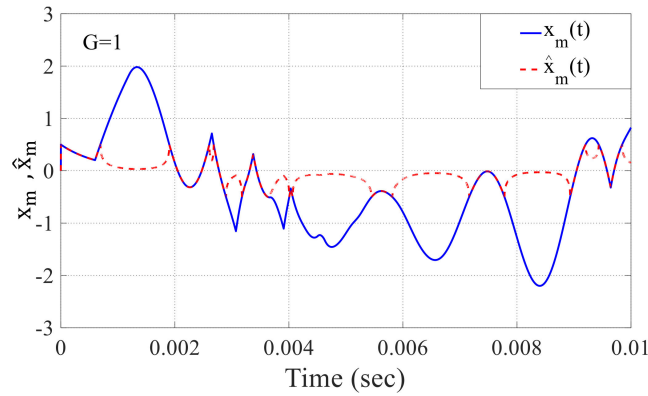
where the phase of  $S_t(t)$  is  $\theta_t$ . The phase difference  $(\theta_t - \theta_v)$  will equal zero if the PLL is locked on the phase of the incoming signal  $\hat{S}_t(t)$ , and the nonlinear (sinusoidal) may be discarded; therefore, the Equation (10) can be rewritten as follows:

$$\hat{v}(t) = G(\theta_t - \theta_v) \tag{11}$$

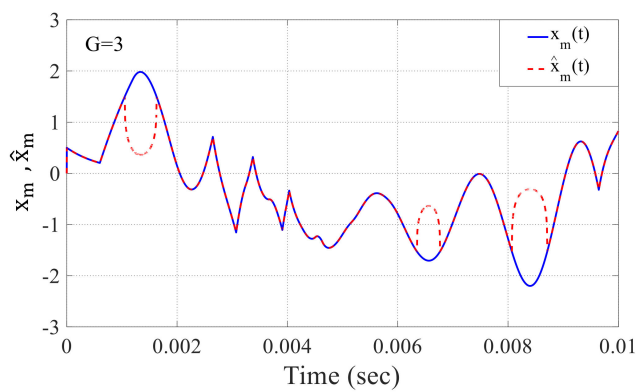
Later, the output from PLL (represented by  $\hat{v}(t)$ ) becomes as an input to another LPF (which is chosen with  $f_{cut} = 1$  MHz, 3rd order, and Butterworth method) to recover  $\hat{x}_m(t)$ . Then, the performance of the proposed continuous chaotic radar system can be measured by

the final output of the correlated over the noisy wireless channel. The correlation qualities are used to assess the chaotic radar’s performance. Thus, the time-delay chaos source (transmitter system) parameter values have been carefully chosen as follows:  $a = 1$ ,  $b = 3$ , and with parameters ( $\tau = 0.6$  ms,  $k = 1500$ ), and the initial condition is set to  $x_m(0) = 0.5$ .

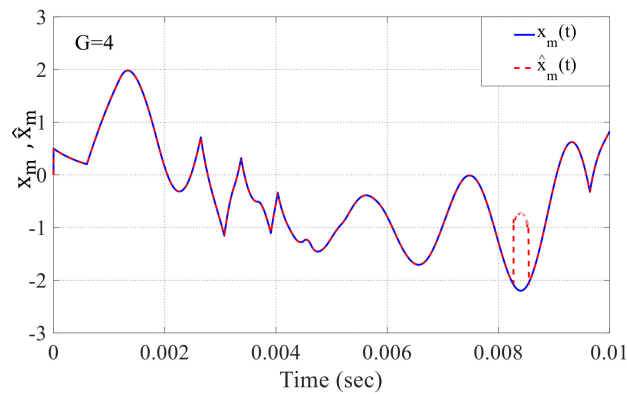
Now, the effect value of the loop gain ( $G$ ) on the recovered signal  $\hat{x}_m(t)$  from the PLL can be seen in Figure 12a–d, where the right  $G$  value must be carefully chosen for the recovered signal  $\hat{x}_m(t)$ . As a result, it is apparent that when the loop gain value becomes 4.6, it has a significant impact on the recovering signal. The resulting signal  $\hat{x}_m(t)$  closely resembles the original signal  $x_m(t)$ .



(a)

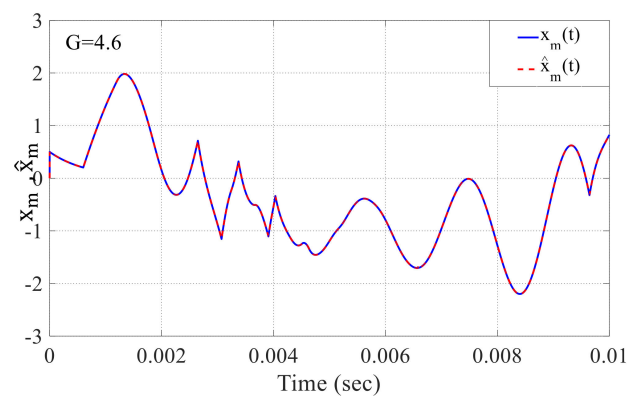


(b)



(c)

Figure 12. Cont.

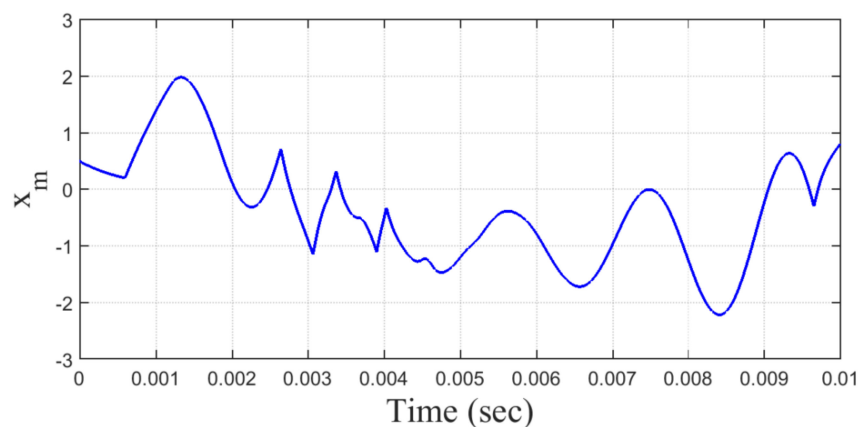


(d)

**Figure 12.** Impact of the loop gain on the recovered signal  $\hat{x}_m(t)$  in the PLL (a)  $G = 1$ , (b)  $G = 3$ , (c)  $G = 4$ , (d)  $G = 4.6$ .

On the other hand, once the PLL locks on the original signal, we will examine the effect of the various noise values on the  $S_t(t)$  over the wireless channel, assuming the sampling frequency,  $f_s = 5$  GHz, and echo delay ( $\tau_d$ ) = 0.2 ns. Upon these assumptions, Figures 13 and 14 show the limited continuous baseband signal  $x_m(t)$  with bandwidth (BW) = 1 MHz and the output signal  $S_t(t)$  from the VCO with a carrier frequency  $f_c = 0.3$  GHz, loop gain  $G = 4.6$ , and  $K_{vco} = 75$  MHz, respectively. Note that the effect of the time delay in Figure 13, for instance  $\tau = 0.6$  ms, shows more chaos dynamics generated in the transmitted FM signal as compared to the counterpart signal in case of  $\tau = 0.5$  ms, depicted in Figure 14. These FM signals are generated using the chaotic attractors obtained in Figure 8a,b.

Furthermore, the correlation performance of the proposed mono-static radar system is also estimated under various values of signal-to-noise ratio (SNR) when VHF (very high frequency) chaotic signal based on FM is considered. Under the effect of noise, the PLL is locked on the phase of the incoming signal  $s_t(t)$ , and the recovered signal  $\hat{x}_m(t)$  disappears when the noise becomes below the value of SNR = -10 dB, as shown in Figure 15e,f. Meanwhile, a clear peak in cross-correlation performance can provide the desired information about the target, as shown in Figure 15a, when SNR = 20 dB.



(a)

**Figure 13.** Cont.

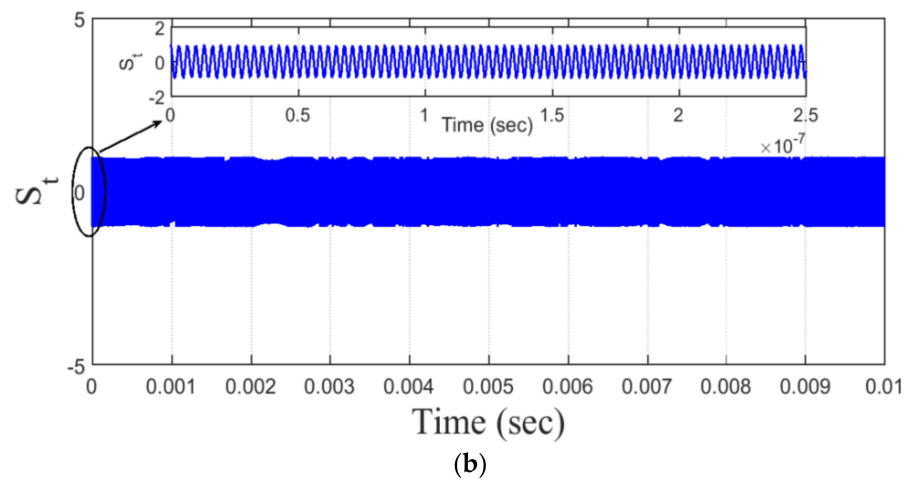


**Figure 13.** Monostatic continuous chaotic radar system for  $\tau = 0.6$  ms and  $x(0) = 0.5, a = 1, b = 3, k = 1500$ . (a)  $x_m(t)$ : the limited chaotic master signal (b)  $s_t(t)$ : the transmitted FM signal.

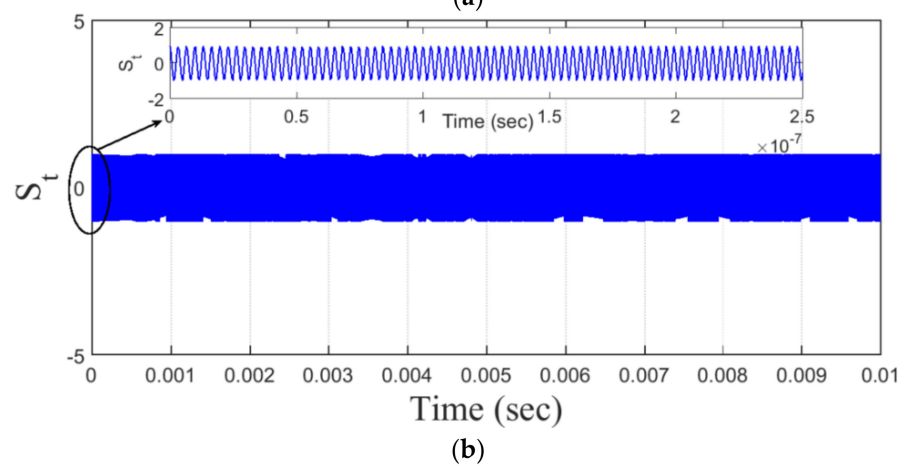
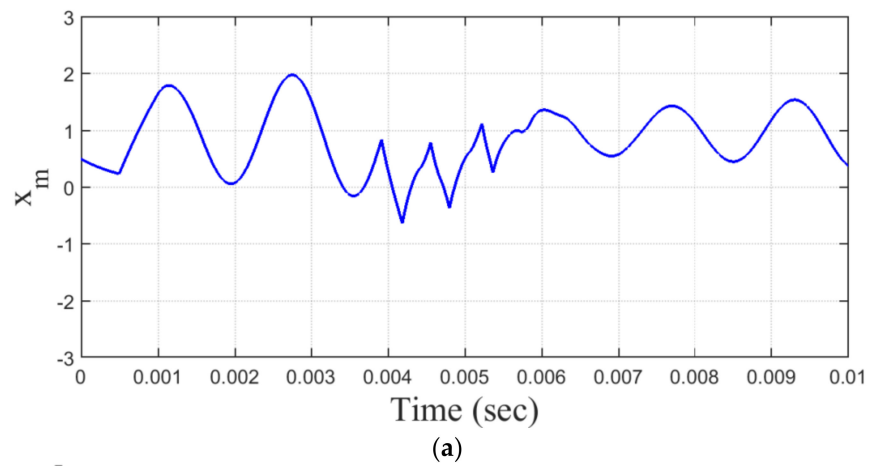


**Figure 14.** Monostatic continuous chaotic radar system for  $\tau = 0.5$  ms and  $x(0) = 0.5, a = 1, b = 3, k = 1500$ . (a)  $x_m(t)$ : the limited chaotic master signal (b)  $s_t(t)$ : the transmitted FM signal.

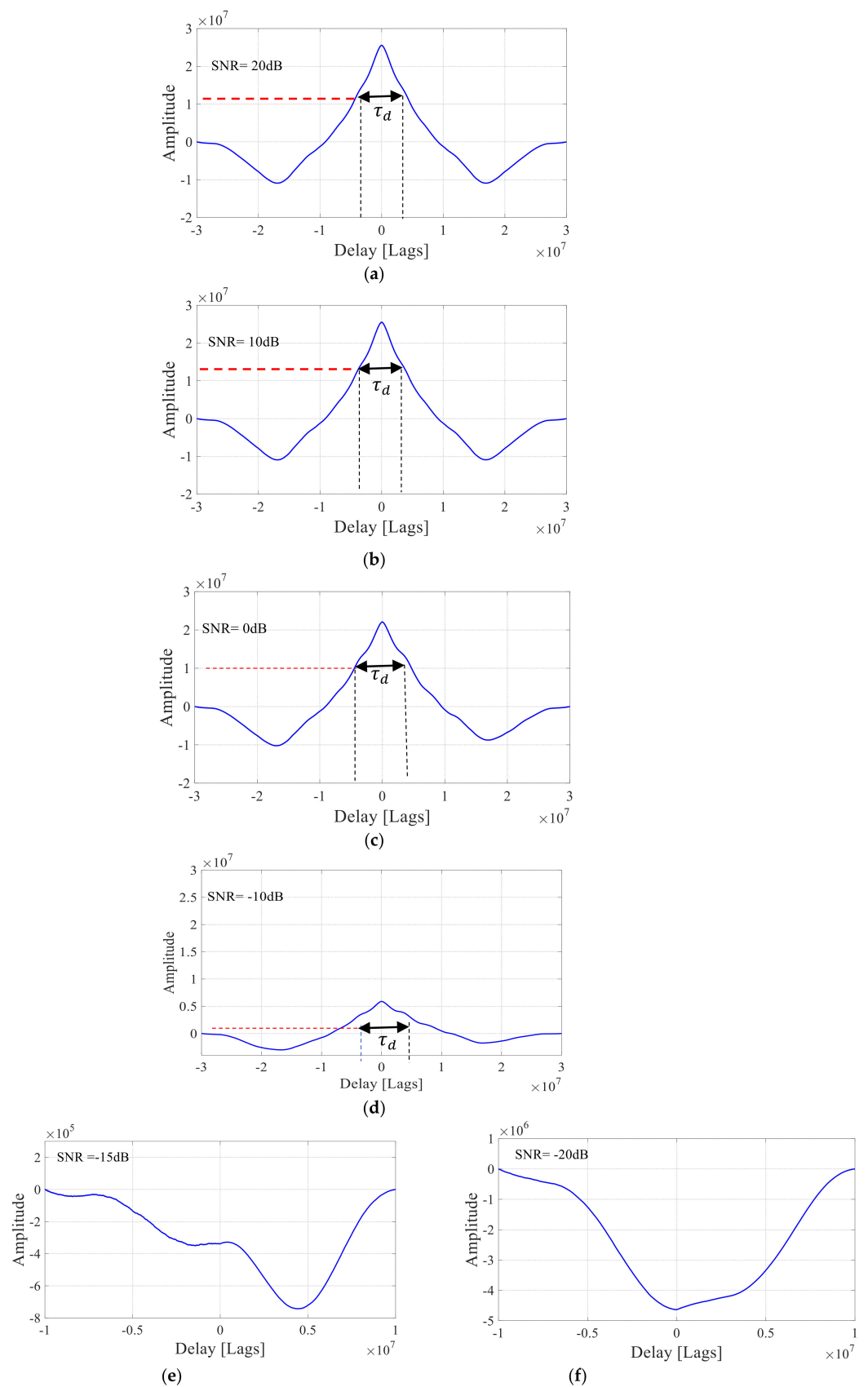


**Figure 15.** The correlation performance of monostatic continuous chaotic radar system for various SNR, (a) SNR = 20 dB, (b) SNR = 10 dB, (c) SNR = 0 dB (d) SNR = -10 dB, no signal: (e) SNR = -15 dB, (f) SNR = -20 dB.

## 7. Comparative Performance with Existing Chaotic Radars

This section clarifies the performance of existing systems in comparison to the time-delay based chaotic radar systems. For example, Table 1 compares the direct time-delay feedback chaotic radar [2] with Colpitts oscillator-based radar [8]. In contrast, Table 2 summarizes the comparison of Indirect FM Chaotic Radars for the proposed time-delay feedback radar versus Lorenz-based Radar [9,10,13]. Likewise, a signal design for generating wideband quasi-Frequency Modulated (FM) waveforms using chaotic systems was also suggested for joint radar-communication (RadComm) systems [37]. However, the receiver design is based on a self-synchronizing chaotic system in place of PLL in order to make fast synchronization and a robust system against the Doppler.

**Table 1.** A comparison example of the direct Chaotic Radars.

Type of Direct Radar	SNR Range	Synch. Type	Parameters Mode	Bandwidth
Based on Colpitts Oscillator [8]	−20 dB	Error Feedback	Match	Wide-band ( $f > 1.6$ GHz)
Based on Time-Delay Feedback [2]	−60 dB −50 dB	Adaptive Observer Pecora and Carroll (PC)	Match and Mismatch	Broadband ( $f < 3$ kHz)

**Table 2.** A comparison of indirect FM Chaotic Radars when a time-delay feedback radar with echo delay = 2 ns.

Indirect Radar	SNR Range	Synch. Type	Bandwidth	Simulation
Lorenz-Based Radar (Bistatic Radar)	6 dB	Pecora & Carroll (PC) (complete)	Wide-band $f_c = 2.5$ GHz, [9]	Advanced Design System (ADS)
	17 dB	Projective	$f_s = 10$ GHz, [10] $B.W = 500$ MHz [13]	
Proposed Time-Delayed Feedback (Monostatic Radar)	−15 dB	Phase Locked Loop (PLL)	Wide-band $f_c = 0.3$ GHz $f_s = 5$ GHz $B.W = 150$ MHz	MATLAB Simulink

Overall, it is noticed that our system based on PLL synchronization can also outperform in terms of low SNR range. It achieves successful recovery at SNR up to −15 dB.

On the other hand, when utilizing Matlab software, it was noticed that the simulation of FM-based time-delay chaotic radar had some problems. In fact, the massive data generated during signal processing (i.e., sampling-interval in ns) led to a storage limitation. Here we set the simulation stop time = 0.07 s to achieve the proper operation. Accordingly, the correlation forms in Figure 15 can exhibit satisfactory peaks but with less resolution; however, in the case of direct chaotic radar [2], once the simulation stop time is set to be 0.5 s, then the correlation peaks become more accurate by 50 times of the FM-based chaotic radar. As a result, one can conclude that more intensive research is needed to eliminate this difficulty in future work in order to create more realistic simulation findings.

## 8. Conclusions and Perspectives

The recent interest in chaos opens more trends to develop different secure applications in radar communication systems. Indeed, the key issue for modern military and civil radars still depends on how to let the radar exhibit more robustness over a wide-band noise. In this paper, to overcome the problems encountered in VLF and other VHF radar systems, such as radar size, large transmission energy, and less precision in range resolution, we developed a new 0.3 GHz indirect mono-static FM-based chaotic system which is based on a time-delay chaotic system. Here, the main contribution is to utilize the Phase-Locked Loop (PLL) for the synchronization process in this radar in order to detect the target's echo



signal accurately under different noise levels and with less design complexity. Thus, the loop gain ( $G$ ) is carefully set when utilizing PLL in this model. This means that the system has been successfully designed with no need to utilize any complete self-synchronization or complex projective synchronization such as adaptive observer to correctly recover the echo signal.

Nevertheless, the effect of sampling interval (in ns) utilized in designing this system begets some restrictions on the signal processing during the simulation process. Therefore, the simulation stop time is set at 0.01 s for proper operation, and hence the robust indirect chaotic radar can be implemented. As a result, such a radar system is considered as one of the state-of-the-art models to detect the target over a high noisy environment and less degradation in the recovered echo signal.

Upon these results, this work can identify some aspects for further study, as follows: (i) The Doppler effect of the echo signal needs more intensive investigation using ambiguity function for moving targets. (ii) To provide a high range resolution, the indirect chaotic radar based on FM can be developed to operate in wider microwave bands (e.g., beyond 1 GHz–3 GHz). Moreover, the different hyperchaotic systems may be also suggested to design monostatic/bi-static radar systems using FPGA. (iii) On the other hand, adaptive control schemes and Artificial Neural Network (ANN) are also eligible to make and predict the synchronization of this time-delayed chaotic system, particularly in secure image encryption/decryption applications.

**Author Contributions:** Conceptualization, M.H.A., G.A.A.-S. and F.R.T.; methodology, M.H.A., G.A.A.-S. and F.R.T.; software, M.H.A. and F.R.T.; validation, M.H.A., G.A.A.-S., F.R.T., S.S.J., K.D. and J.A.; formal analysis, F.R.T., G.A.A.-S. and M.H.A.; investigation, G.A.A.-S., F.R.T. and M.H.A.; resources, M.H.A., G.A.A.-S., F.R.T., A.M.A.A., H.A.A., J.A. and S.S.J.; writing—original draft preparation, M.H.A., G.A.A.-S. and F.R.T.; writing—review and editing, G.A.A.-S., M.H.A., A.M.A.A., J.A., K.D. and S.S.J.; visualization, G.A.A.-S., M.H.A., F.R.T., S.S.J., K.D. and J.A.; supervision, G.A.A.-S. and F.R.T.; project administration, G.A.A.-S. and F.R.T.; funding acquisition, S.S.J., K.D. and J.A. All authors have read and agreed to the published version of the manuscript.

**Funding:** This research received no external funding.

**Data Availability Statement:** Not applicable.

**Acknowledgments:** One of the authors, Sajjad Shaukat Jamal, extends his gratitude to the Deanship of Scientific Research at King Khalid University for funding this work through a research groups program under grant number R. G. P. 2/86/43.

**Conflicts of Interest:** The authors declare no conflict of interest.

## References

1. Dao, H.; Rodgers, J.C.; Murphy, T.E. Chaotic Dynamics of a Frequency-Modulated Microwave Oscillator with Time-Delayed Feedback. *Chaos Interdiscip. J. Nonlinear Sci.* **2013**, *23*, 013101. [[CrossRef](#)] [[PubMed](#)]
2. Al-Suhail, G.A.; Tahir, F.R.; Abd, M.H.; Pham, V.T.; Fortuna, L. Modelling of Long-Wave Chaotic Radar System for Anti-Stealth Applications. *Commun. Nonlinear Sci. Numer. Simul.* **2018**, *57*, 80–96. [[CrossRef](#)]
3. Bin, C.; Jun, T.; Yong, Z.; Peng, C.; Jian, H.; Qiang, H.G. Chaotic Signals with Weak-Structure Used for High Resolution Radar Imaging. In Proceedings of the 2009 WRI International Conference on Communications and Mobile Computing, Kunming, China, 6–8 January 2009; pp. 325–330.
4. Pappu, C.S.; Beal, A.N.; Flores, B.C. Chaos Based Frequency Modulation for Joint Monostatic and Bistatic Radar-Communication Systems. *Remote Sens.* **2021**, *13*, 4113. [[CrossRef](#)]
5. Curry, G.R. *Radar System Performance Modeling*, 2nd ed.; Artech House: Boston, MA, USA; London, UK, 2004; 410p.
6. Kapur, V. *Stealth Technology and Its Effect on Aerial Warfare*; Institute for Defence Studies and Analyses: New Delhi, India, 2014; p. 33.
7. Shi, Z.G.; Qiao, S.; Chen, K.; Cui, W.Z.; Ma, W.; Jiang, T.; Ran, L.X. Ambiguity Functions of Direct Chaotic Radar Employing Microwave Chaotic Colpitts Oscillator. *Prog. Electromagn. Res.* **2007**, *77*, 1–14. [[CrossRef](#)]
8. Qiao, S.; Jiang, T.; Ran, L.X.; Chen, K. Ultra-Wide Band Noise-signal Radar Utilizing Microwave Chaotic Signals and Chaos Synchronization. *PIERS Online* **2007**, *3*, 1326–1329. [[CrossRef](#)]
9. Pappu, C.S.; Flores, B.C.; Debroux, P. Analysis of the Ambiguity Function for an FM Signal Derived from the Lorenz Chaotic Flow. In Proceedings of the SPIE Defense, Security and Sensing, Baltimore, MD, USA, 23–27 April 2012; Volume 8361, pp. 366–377.

10. Pappu, C.S.; Verdin, B.; Flores, B.C.; Boehm, J.; Debroux, P. Analysis of Chaotic FM System Synchronization for Bistatic Radar. In Proceedings of the SPIE Defense + Security, Baltimore, MD, USA, 17–21 April 2015; Volume 9461, pp. 309–319.
11. Liu, L.; Hu, J.; Li, H.; Li, J.; He, Z.; Han, C. A Noise Resistant Synchronization Method and Its Application in Chaotic Radar. In Proceedings of the IEEE CIE International Conference on Radar, Chengdu, China, 24–27 October 2011; Volume 2, pp. 1884–1886.
12. Zhong, D.; Xu, G.; Luo, W.; Xiao, Z. Real-time multi-target ranging based on chaotic polarization laser radars in the drive-response VCSELs. *Opt. Express* **2017**, *25*, 21684–21704. [[CrossRef](#)]
13. Pappu, C.S.; Flores, B.C.; Debroux, P.S.; Verdin, B.; Boehm, J. Synchronisation of bistatic radar using chaotic AM and chaos-based FM waveforms. *IET Radar Sonar Navig.* **2017**, *11*, 90–97. [[CrossRef](#)]
14. William, A. Wireless Communication of a Chaotic Waveform. Master's Thesis, Auburn University, Auburn, AL, USA, 2015.
15. Zikidis, K.; Skondras, A.; Tokas, C. Low Observable Principles, Stealth Aircraft and Anti-Stealth Technologies. *J. Comput. Model.* **2014**, *4*, 129–165.
16. Liu, C.; Li, C.; Li, C. Quasi-Synchronization of Delayed Chaotic Systems with Parameters Mismatch and Stochastic Perturbation. *Commun. Nonlinear Sci. Numer. Simulat.* **2011**, *16*, 4108–4119. [[CrossRef](#)]
17. Zhen, J. Linear Generalized Synchronization of Chaotic Systems with Uncertain Parameters. *J. Syst. Eng. Electron.* **2008**, *19*, 779–784. [[CrossRef](#)]
18. Pogromsky, A.; Nijmeijer, H. Observer-Based Robust Synchronization of Dynamical Systems. *Int. J. Bifurc. Chaos* **1998**, *8*, 2243–2254. [[CrossRef](#)]
19. He, W.; Qian, F.; Han, Q.; Cao, J. Lag Quasi-Synchronization of Coupled Delayed Systems with Parameter Mismatch. *IEEE Trans. Circuits Syst. I Regul. Pap.* **2011**, *58*, 1345–1357. [[CrossRef](#)]
20. Huang, T.; Li, C.; Liao, X. Synchronization of a Class of Coupled Chaotic Delayed Systems with Parameter Mismatch. *Chaos Interdiscip. J. Nonlinear Sci.* **2007**, *17*, 033121. [[CrossRef](#)]
21. Cuomo, K.M.; Oppenheim, A.V.; Strogatz, S.H. Synchronization of Lorenz-Based Chaotic Circuits with Applications to Communications. *IEEE Trans. Circuits Syst.* **1993**, *40*, 626–633. [[CrossRef](#)]
22. Ott, E.; Grebogi, C.; Yorke, J.A. Controlling chaos. *Phys. Rev. Lett.* **1990**, *64*, 1196–1199. [[CrossRef](#)]
23. Yau, H.T. Design of Adaptive Sliding Mode Controller for Chaos Synchronization with Uncertainties. *Chaos Solitons Fractals* **2004**, *22*, 341–347. [[CrossRef](#)]
24. Lian, K.Y.; Liu, P.; Chiang, T.S.; Chiu, C.S. Adaptive Synchronization Design for Chaotic Systems via a Scalar Driving Signal. *IEEE Trans. Circuits Syst. I Fundam. Theory Appl.* **2002**, *49*, 17–27. [[CrossRef](#)]
25. Itoh, M.; Yang, T.; Chua, L.O. Conditions for Impulsive Synchronization of Chaotic and Hyperchaotic Systems. *Int. J. Bifurc. Chaos* **2001**, *11*, 551–560. [[CrossRef](#)]
26. Tan, X.; Zhang, J.; Yang, Y. Synchronizing chaotic systems using backstepping design. *Chaos Solitons Fractals* **2003**, *16*, 37–45. [[CrossRef](#)]
27. Yu, X.; Song, Y. Chaos Synchronization via Controlling Partial State of Chaotic Systems. *Int. J. Bifurc. Chaos* **2001**, *11*, 1737–1741. [[CrossRef](#)]
28. Ge, C.; Wang, H. Synchronization Criteria of Chaos Systems with Time-Delay Feedback Control. *Int. J. Comput. Sci. Issues* **2013**, *10*, 749–753.
29. Wang, L.; Jiang, S.; Ge, M.F.; Hu, C.; Hu, J. Finite-/Fixed-Time Synchronization of Memristor Chaotic Systems and Image Encryption Application. *IEEE Trans. Circuits Syst. I Regul. Pap.* **2021**, *68*, 4957–4969. [[CrossRef](#)]
30. Tahir, F.R.; Al-Suhail, G.A.; Abd, M.H. String of scrolls from a time-delayed chaotic circuit. *Int. J. Simul. Process Model.* **2018**, *13*, 463–472. [[CrossRef](#)]
31. Buscarino, A.; Fortuna, L.; Frasca, M.; Sciuto, G.; Xibilia, M.G. Design of Time-Delay Chaotic Electronic Circuits. *IEEE Trans. Circuits Syst. I Regul. Pap.* **2011**, *58*, 1888–1896. [[CrossRef](#)]
32. Buscarino, A.; Fortuna, L.; Frasca, M.; Sciuto, G.; Xibilia, M.G. Harmonic balance method for time-delay chaotic systems design. *IFAC Proc. Vol.* **2011**, *44*, 5112–5117. [[CrossRef](#)]
33. Abd, M.H.; Tahir, F.R.; Al-Suhail, G.A.; Pham, V.T. An adaptive observer synchronization using chaotic time-delay system for secure communication. *Nonlinear Dyn.* **2017**, *90*, 2583–2598. [[CrossRef](#)]
34. Li, C.; Thio, W.J.C.; Iu, H.H.C.; Lu, T. Memristive Chaotic Oscillator with Increasing Amplitude and Frequency. *IEEE Access* **2018**, *6*, 12945–12950. [[CrossRef](#)]
35. Bianchi, G.; Kuznetsov, N.V.; Leonov, G.A.; Yuldashev, M.V.; Yuldashev, R.V. Limitations of PLL simulation: Hidden oscillations in Matlab and SPICE. In Proceedings of the International Congress on Ultra Modern Telecommunications and Control Systems and Workshops (ICUMT), Brno, Czech Republic, 6–8 October 2015; pp. 79–84.
36. Pappu, C.S.; Carroll, T.L.; Flores, B.C. Simultaneous Radar-Communication Systems Using Controlled Chaos-Based Frequency Modulated Waveforms. *IEEE Access* **2020**, *8*, 48361–48375. [[CrossRef](#)]
37. Pappu, C.S.; Carroll, T.L. Quasi-FM Waveform Using Chaotic Oscillator for Joint Radar and Communication Systems. *Chaos Solitons Fractals* **2021**, *152*, 111449. [[CrossRef](#)]